AIP | Applied Physics Letters

Optical geometries for fiber-based organic photovoltaics

Jiwen Liu, Manoj A. G. Namboothiry, and David L. Carroll

Citation: Appl. Phys. Lett. **90**, 133515 (2007); doi: 10.1063/1.2716864
View online: http://dx.doi.org/10.1063/1.2716864
View Table of Contents: http://apl.aip.org/resource/1/APPLAB/v90/i13
Published by the AIP Publishing LLC.

Optical geometries for fiber-based organic photovoltaics

Jiwen Liu, Manoj A. G. Namboothiry, and David L. Carroll[a)]
The Center for Nanotechnology and Molecular Materials, Department of Physics, Wake Forest University, Winston-Salem, North Carolina 27109

(Received 29 November 2006; accepted 20 February 2007; published online 30 March 2007)

Poly(3-hexylthiophene):1-(3-methoxycarbonyl)-propyl-1-phenyl-(6,6)C_{61} photovoltaic devices were fabricated as a cladding onto large diameter optical fibers. The performance of the devices was dependent on fiber diameter as well as the angle of incidence of light onto the cleaved fiber face. The authors suggest that absorption by the active layer is dominated by different mechanisms at different angles: evanescent coupling of the light at small incident angles and far field scattering of the light from the fiber at higher angles. Further, a comparison of devices that only partially clad the fiber to those that fully clad suggests the formation of confined radiation modes. © *2007 American Institute of Physics*. [DOI: 10.1063/1.2716864]

Typically, organic thin film photovoltaics were fabricated with their active (absorbing) layers too thin to effectively absorb incident light. That is, flat, thin film architectures were primarily intended to aid in the removal of low mobility charge, but they provide for poor optical coupling.[1–8] Ideally, if the radiant energy could be "waveguided" into organic thin film devices such that reflective and transmissive losses were minimized while keeping the electronic properties the same, the efficiencies could be raised significantly. In this work, we examine geometric optical considerations of coupling light into thin, organic active layers that are alternative to the typical thin film structures used in photovoltaics. Utilizing standard multimode optical fibers, we have fabricated thin film devices which we refer to as "claddings" based on the bulk heterojunction blend poly(3-hexylthiophene):1-(3-methoxycarbonyl)-propyl-1-phenyl-(6,6)C_{61} (P3HT: PCBM) as an absorbing material and indium tin oxide (ITO) as the transparent conductor. Surprisingly, this architecture works with active film thicknesses significantly greater than those typical for thin film devices, suggesting that propagating modes within the layer are playing a role in the performance of the device. We envisage these fiber devices as the building blocks for higher performance organic platforms.

Multimode solid core fibers were used to fabricate the fiber devices, there are two steps. First, the jacket of multimode fibers (BFH37, high OH, from 1.5 to 0.2 mm, from Thorlabs) was stripped off and the hard polymer cladding was removed. Then the core of the fiber was cleaned in an ultrasonic bath with de-ionized water, acetone, and isopropyl alcohol successively for 20 min and dried in an oven for 15 min at 100 °C. Finally, the cleaned fiber was coated with indium tin oxide (In/Sn=90:10) by a dip coating procedure using metal salts to form a sol gel as described by Ramanan.[9] Finally the gel was densified through annealing to form a highly conductive (100 Ω/cm) optical fiber.

The second step is the fabrication of the device on the conductive fiber. The ITO coated fibers were thoroughly cleaned in an ultrasonic bath with acetone and isopropyl alcohol successively for 20 min and dried in oven at 100 °C. The fibers were then exposed to ozone for 90 min (rotating the fiber three times every after 30 min). Poly(3,4-ethylene dioxythiophene):poly(styrene sulfonate) (PEDOT:PSS) solution (Baytron P) was then deposited by dip coating and dried at 100 °C for 15 min (the thickness of the PEDOT:PSS film is ~150 nm). Subsequently, a solution of P3HT:PCBM =1:0.8 in chlorobenzene was deposited on the fiber through dip coating (the thickness of the polymer film is ~300 nm). Finally, LiF and Al electrodes were deposited via thermal evaporation at the pressure of 10^{-6} torr. The thickness of LiF is around 0.3–0.4 nm, and the thickness of Al film is 100 nm. The length of the fiber with active area for most of our studies was about 1.4 cm. The resulting device structure is shown in Fig. 1. Thirty devices of each diameter were made for comparison and consistency.

We note that the overall quality of the thin films used in this work was not very high which is surprising considering how well the devices function. Atomic force microscopy was used to characterize surface roughness of the ITO layer as

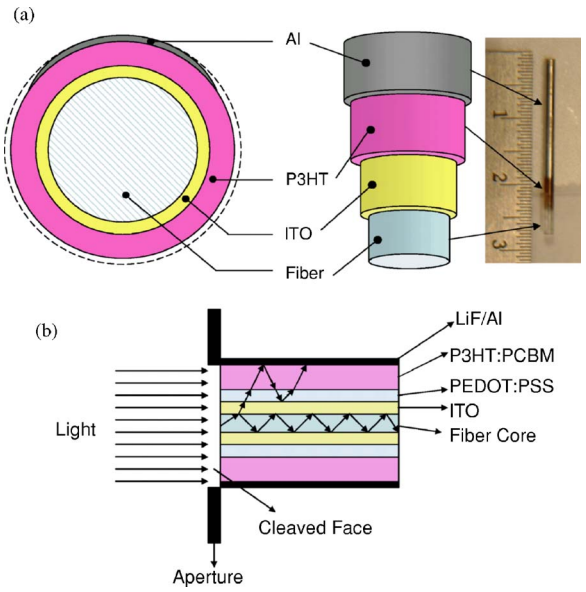

FIG. 1. (Color online) (a) Schematic of the fiber photovoltaic cell architecture and (b) light illumination, ray diagram of light propagation, confinement of light inside the active medium through reflection from Al, and refractive index difference between the layers.

a)Author to whom correspondence should be addressed; electronic mail: carroldl@wfu.edu

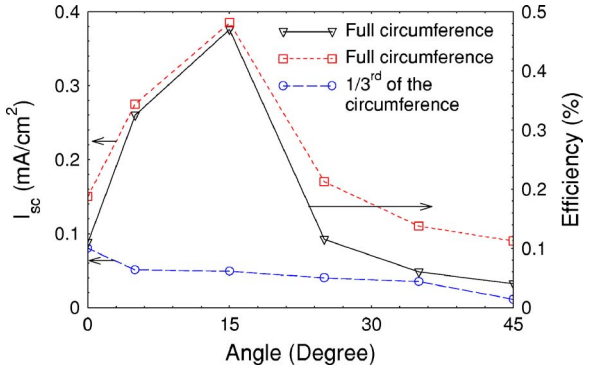

FIG. 2. (Color online) Comparison of the I_{sc} for full circumference coated with LiF/Al and 1/3 of circumference coated with LiF/Al on fiber and power conversion efficiency as a function of the angle of incidence with respect to the axis of the optical fiber of fiber diameter of 1.5 mm.

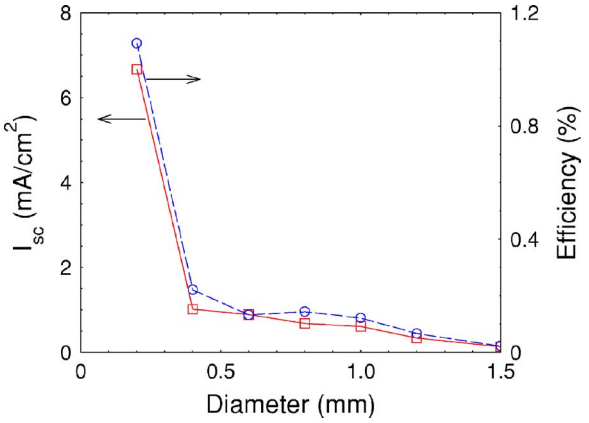

FIG. 3. (Color online) Comparison of the I_{sc} and power conversion efficiency as a function of the fiber diameter for light incident along the axis and perpendicular to the plane of the cleaved surface of the fiber (only 1/3 of the fiber circumference is coated with LiF/Al electrode).

well as the polymer layers at different stages during fabrication. Large aggregated features of fractions of a micron were observed in the ITO and PEDOT:PSS layers (not shown). These were reflected in the final device on the outer metallic layer. Notice again the roughness of the layer compared with the mirror smooth metal finish normally seen in spun cast and evaporated thin film devices.

Devices were tested using an AM1.5g standard (Oriel) operating with an illumination intensity of 100 mW/cm^2. This is the equivalent of one sun illuminating the cleaved end of the fiber. The illumination was made along the axis of the fiber and perpendicular to the plane of the cleaved surface [Fig. 1(b)]. Apertures of appropriate diameters corresponding to the fiber diameter were used at the cleaved surface to eliminate illumination from the side of the device Our system's solar mismatch factor of 10% was determined using a calibrated standard diode, as well as a direct comparison with a National Renewable Energy Laboratory certified simulator. Current voltage characteristics were collected using Keithley 236 source-measurement unit. Contacts were silver pasted onto the fiber and the fiber was held rigid during testing.

Most of our test devices were fabricated with the outer LiF/Al electrode covering 1/3 of the circumference (confirmed by optical microscopy) on P3HT:PCBM by thermal evaporation. This was done for ease of fabrication when using the smallest diameter fibers. A schematic of device architecture is shown in Fig. 1. While coating the whole outer fiber is difficult for the smallest fibers with our current setup, it could be done for larger diameter fibers and so we can understand the overall effect through a direct comparison as shown in Fig. 2. Here we compare the short circuit current density (I_{sc}) for two 1.5 mm diameter fibers, one fully coated with metal and the other coated on only 1/3 of the circumferences of the device. The I_{sc} was computed by dividing the total current produced by the device by the illuminated area: π(radius of fiber)^2, which is the cross sectional area at the cleaved surface, perpendicular to the axis of the optical fiber. Notice that we compare the structure's performance here as a function of incident angle of illumination on the cleaved face of the fiber. That is, the angle at which the incoming light is incident is varied from 0° (along the axis of the fiber) to 45° to the axis of the fiber. The functional dependence of the current produced by fiber devices is clearly different for fully coated and 1/3 circumference coated fibers. Most pronounced is the sharp increase in I_{sc} observed for incident (coupling) angles of about 15° in fully coated fibers but not seen in the fibers with only 1/3 circumference area contact. We suggest that this is likely due to the reflective nature of the Al contact which effectively confines the radiation into the cladding. For small incident angles, light is coupled into the device primarily through the evanescent field. This results in more than double the I_{sc} from the fully coated fiber at normal incidence, since there is more contact area to collect the current produced in the absorber. However, as the incident angle is increased there are more refractive losses into the cladding. The majority of the power in these propagating modes is lost (90%) in the partially contacted fiber because it is not efficiently absorbed in the thin cladding and the light is transmitted out of the structure. Further, for the light that is absorbed, radiative recombination dominates the cladding where there is no contact. This is not the case when a full cladding is added, as both the refracted rays and the power from radiative recombination are reflected by the Al sheath back into the structure [Fig. 1(b)]. For the largest angles, we observe that reflection from the front surface of the fiber is becoming large and 60% of the light is lost due to poor coupling. While this is a rather simple picture of the complex optical system in fiber architectures, it is useful in suggesting how the contacts of this structure have an effect beyond that of increasing the effective collection area of the absorber. In other words, the difference between three contacts and one contact on the fiber is more than simply multiplying the current by 3.

The I_{sc} produced at standard illumination, at normal angle of incidence, is shown for decreasing fiber diameters using only one contact in Fig. 3. I_{sc} in the device increases significantly as the diameter of the fiber is decreased. The I_{sc} is quite low for the devices fabricated from 1.5 mm fibers, 0.09 (±0.05) mA/cm^2. This is reasonable since in the large multimode fiber, only a small fraction of the power being transmitted by the fiber is lost at the fiber-cladding interface, most is transmitted straight through the back. As the fiber diameter is decreased, however, the numerical aperture of the fiber changes and refractive losses into the cladding increase. By simply decreasing the diameter to 1200 μm, we get an increase of I_{sc} to 0.4 (±0.3) mA/cm^2 and decreasing further to 600 μm, the I_{sc} current rises to 0.9 (±0.3) mA/cm^2. This smooth increase is interrupted, however, as we decrease the

fiber to 200 μm where we achieve an astonishing 7.0 ($\pm$2.5) mA/cm^2. We note that for the smallest diameter devices, variation from device to device is rather high because of the difficulty in maintaining film quality on the small fibers. For the currents given above, many devices were measured and the variations are given in parenthesis.

From the above argument, to estimate the *minimum* performance of the fully coated device, we can multiply the current by the added surface area. Doing so, for the highest current densities we have measured for a device contact of 1/3 of the circumference of the fiber, we achieve current densities of approximately 28 mA/cm^2. We note that for the spectral overlap of P3HT absorber used in these devices, the integrated photon flux gives a maximum of approximately 30 mA/cm^2, suggesting an extremely high internal conversion efficiency.[8] We further note that we expect this to be the ultimate limit in the fiber architecture as well. To see how these expectations translate into efficiency performance, we plot the efficiency for the fiber devices as a function of fiber diameter in Fig. 3. These are calculated by determining current densities described above and taking the V_{oc} and filling factor ($=I_{max}V_{max}/I_{sc}V_{oc}$) for each device and plotting the average. $\eta_{external}=I_{sc}\,V_{oc}\mathrm{FF}/P_{incident}$, where I_{sc} is the short circuit current, V_{oc} is the open circuit voltage, FF is the filling factor calculated from the *IV* curves by taking the maximum power rectangle, and $P_{incident}$ is the power density of the incoming light.[10] Recall that we have apertured the system to eliminate side illumination. We note again that these do not represent the best values possible, since we use only the 1/3 circumference contact devices for these tests and do not multiply by the addition area for Fig. 3. Notice that the smallest diameter fiber produces nearly 1.1% efficiency (or 3.3% for fully contacted devices) in normal incidence. Off incidence this is clearly higher. Further, in terms of the use of these devices in solar cell applications, the angle of incidence dependence works very much in the favor of increased average performance as we show in Fig. 2 for a 1.5 mm diameter fiber device. Finally, due to variations in film quality there is significant variation in V_{oc} for the small diameter devices. We show the poorest performance of the device set here.

We have demonstrated a fiber-based architecture for use in organic photovoltaics. This device utilizes a thin film absorbing layer with ITO and Al electrodes as a cladding. Device power conversion efficiency is dependent on optical coupling and coating techniques. This, we suggest, comes from confined radiation modes within the active layer that are responsible for the high level of conversion efficiency in this architecture.

The authors would like to acknowledge AFOSR Grant No. FA9550-04-1-0161 for funding this work.

[1] S. A. Mcdonald, G. Konstantatos, S. Zhang, P. W. Cyr, E. J. D. Klem, L. Levina, and E. H. Sargent, Nat. Mater. **4**, 138 (2005).
[2] C. J. Brabec, N. S. Sariciftci, and J. C. Hummelen, Adv. Funct. Mater. **11**, 15 (2001).
[3] C. J. Brabec, Sol. Energy Mater. Sol. Cells **83**, 273 (2004).
[4] M. A. Green, Prog. Photovoltaics **13**, 85 (2005).
[5] R. J. Ellingson, M. C. Beard, J. C. Johnson, P. Yu, O. I. Micic, A. J. Nozik, A. Shabaev, and A. L. Efros, Nano Lett. **5**, 865 (2005).
[6] M. R. Reyes, K. Kim, and D. L. Carroll, Appl. Phys. Lett. **87**, 83506 (2005).
[7] M. R. Reyes, K. Kim, J. Dewald, R. L. Sandoval, A. Avadhanula, S. Curran, and D. L. Carroll, Org. Lett. **7**, 5749 (2005).
[8] F. Yang, M. Shtein, and S. R. Forrest, Nat. Mater. **4**, 37 (2005).
[9] S. R. Ramanan, Thin Solid Films **389**, 207 (2001).
[10] C. Brabec, V. Dyakonov, J. Parisi, and N. S. Sariciftci, *Organic Photovoltaics: Concepts and Realizations*, Springer Series in Materials Science Vol. 60 (Springer, Berlin, 2003), p. 178.